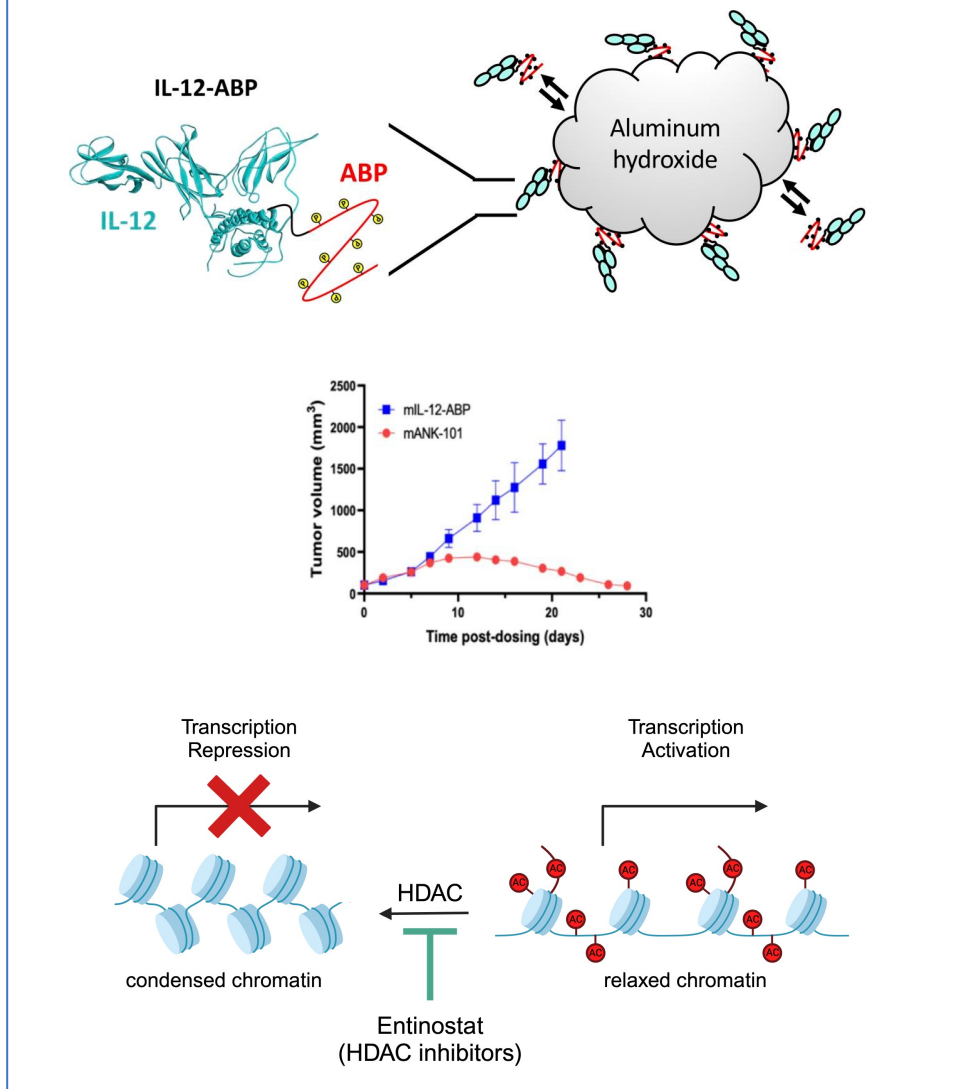


BACKGROUND

Background: Clinical resistance to immune checkpoint blockade (ICB) is prevalent across solid malignancies, thus prompting the need for novel therapies. Interleukin-12 (IL-12) is an important cytokine for cancer immunotherapy due to its ability to bridge innate and adaptive immunity^{1,2}. However, the narrow therapeutic index and toxicity associated with systemic IL-12 administration has hampered its clinical development. ANK-101 is an alum-anchored human IL-12 providing tumor retention upon intra-tumoral delivery³. In this study, we investigated the anti-tumor activity and mechanism of action of murine ANK-101 (mANK-101) delivered intra-tumorally in combination with the class I histone deacetylase (HDAC) inhibitor entinostat, in different ICB-refractory murine tumor models, including CT26 (colorectal) and MOC-1 (HPV16^{neg} head and neck).



MATERIALS AND METHODS

Reagents: Entinostat and mANK-101 were kindly provided by Syndax and Ankyra, respectively, under Cooperative Research and Development Agreements (CRADA) with the NCI. A sub-optimal dose of mANK-101 (2 µg) has been chosen to explore the combination potential of mANK-101 with entinostat. Low-fat diet of 35% sucrose was enriched with entinostat for a target daily dose of 6 mg/kg (Research Diets). Anti-mouse CD8α (clone 2.43), CD4 (GK1.5), and NK1.1 (PK136) antibodies were purchased from BioXCell.

Methods (in brief): Mice receiving entinostat diet and/or mANK-101 were monitored for anti-tumor activity, survival and protective memory. The contribution of CD8⁺, CD4⁺, and NK lymphocytes to antitumor effects were investigated via immune depletion. Analysis of tumor-specific T cell responses and comprehensive proteomic, transcriptomic, and tumor architecture analysis of the immunome was performed in MOC-1 tumors, tumor-draining lymph node (tdLN), and spleen. In addition, functional analysis of CD8⁺ T cells in the periphery were performed.

Statistics: Bar graphs and violin plots show mean ± SEM with one-way ANOVA and Tukey's multiple comparisons; tumor volumes show two-way ANOVA with multiple comparisons; survivals show Mantel-cox; all data except scRNAseq is representative of 2 or 3 independent experiments. ns=not significant, *P<0.05, **P<0.01, ***P<0.001, ****P<0.0001. All schemas were created with BioRender.com.

RESULTS

1 mANK-101 synergizes with Entinostat to suppress CT26 and MOC-1 tumors, eliciting protective memory and increasing survival

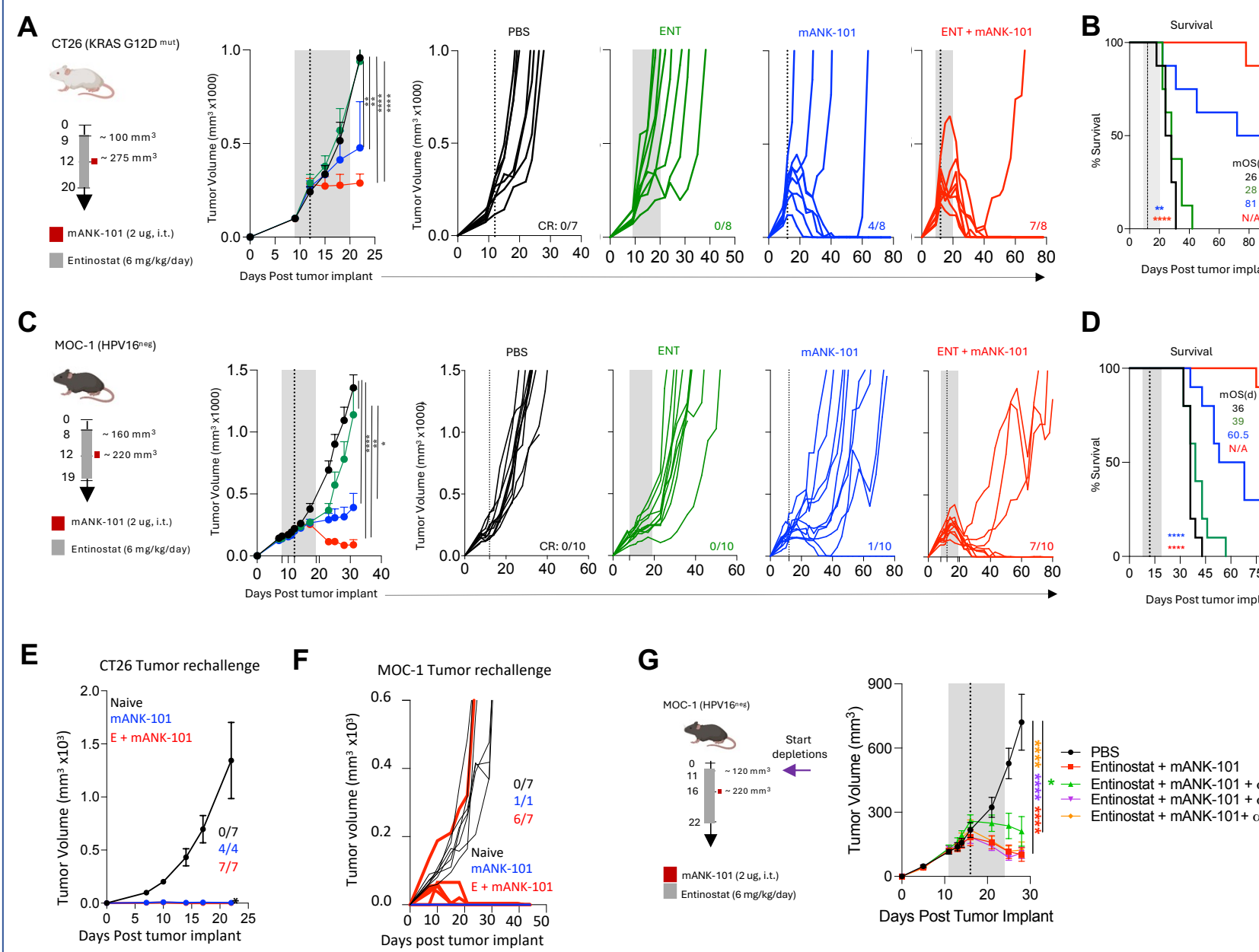


Figure 1. (A) Aggregate and individual tumor growth curves with cure rates (CR) in CT26 tumor-bearing mice. (B) Graph displaying % survival and median overall survival (mOS) for CT26 tumor-bearing mice. (C) Aggregate and individual tumor growth curves with CR in MOC-1 tumor-bearing mice. (D) Graph displaying % survival and mOS for MOC-1 tumor-bearing mice. (E) Tumor growth curves of naive or CT26 cured mice rechallenged with matching tumor cells. (F) Tumor growth curves of naive or MOC-1 cured mice rechallenged with matching tumor cells. (G) MOC-1 depletion study schematic and associated tumor growth curves for mANK-101 plus entinostat combination-treated mice with and without depletion antibodies. Dotted lines: mANK-101 dosing; grey bar: Entinostat diet; mOS = Median overall survival (days).

2 Combination therapy elicits a pro-inflammatory environment in the periphery and induces abscopal anti-tumor activity in MOC-1 tumors

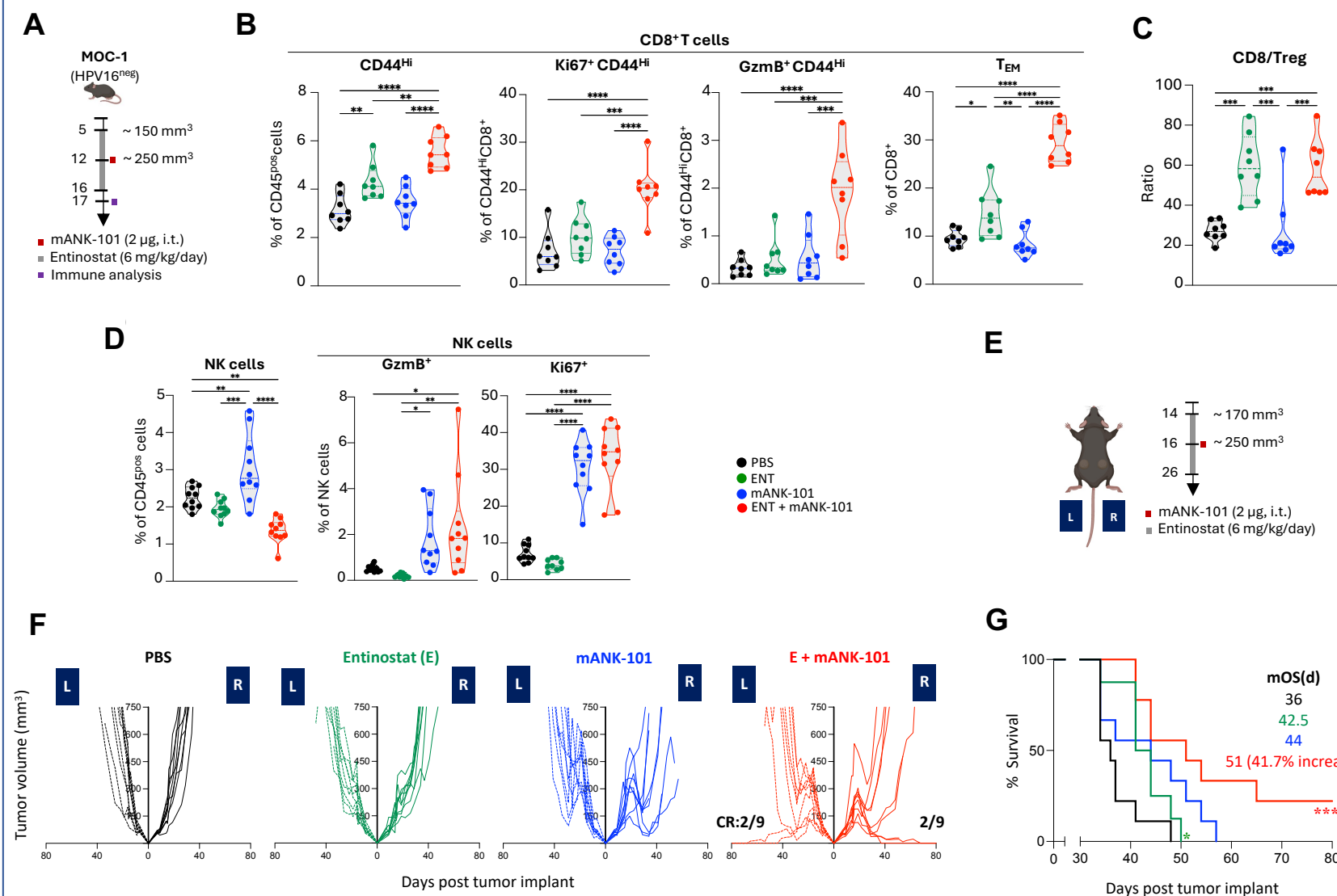


Figure 2. (A) MOC-1 tumor-bearing mice were treated as shown and sacrificed on Day 17 for immune analysis. (B) Quantification of activated CD8⁺ T cells that are proliferative (Ki67⁺) and cytolytic (GzmB⁺) in the spleen. (C) Quantification of IFNγ in sera. (D) Number of NK cell populations in the spleen. (E) Schematic of MOC-1 HPV16^{neg} abscopal study. (F) Individual tumor growth curves from treated (Right, R) and untreated (Left, L) tumors, with cure rates (CR). (G) Graph displaying % survival and median overall survival (mOS) for MOC-1 abscopal study. Dotted lines: mANK-101 dosing; grey bar: Entinostat diet

3 Combination therapy creates a pro-inflammatory environment in the TME increasing CD8⁺ T cell infiltration and activation

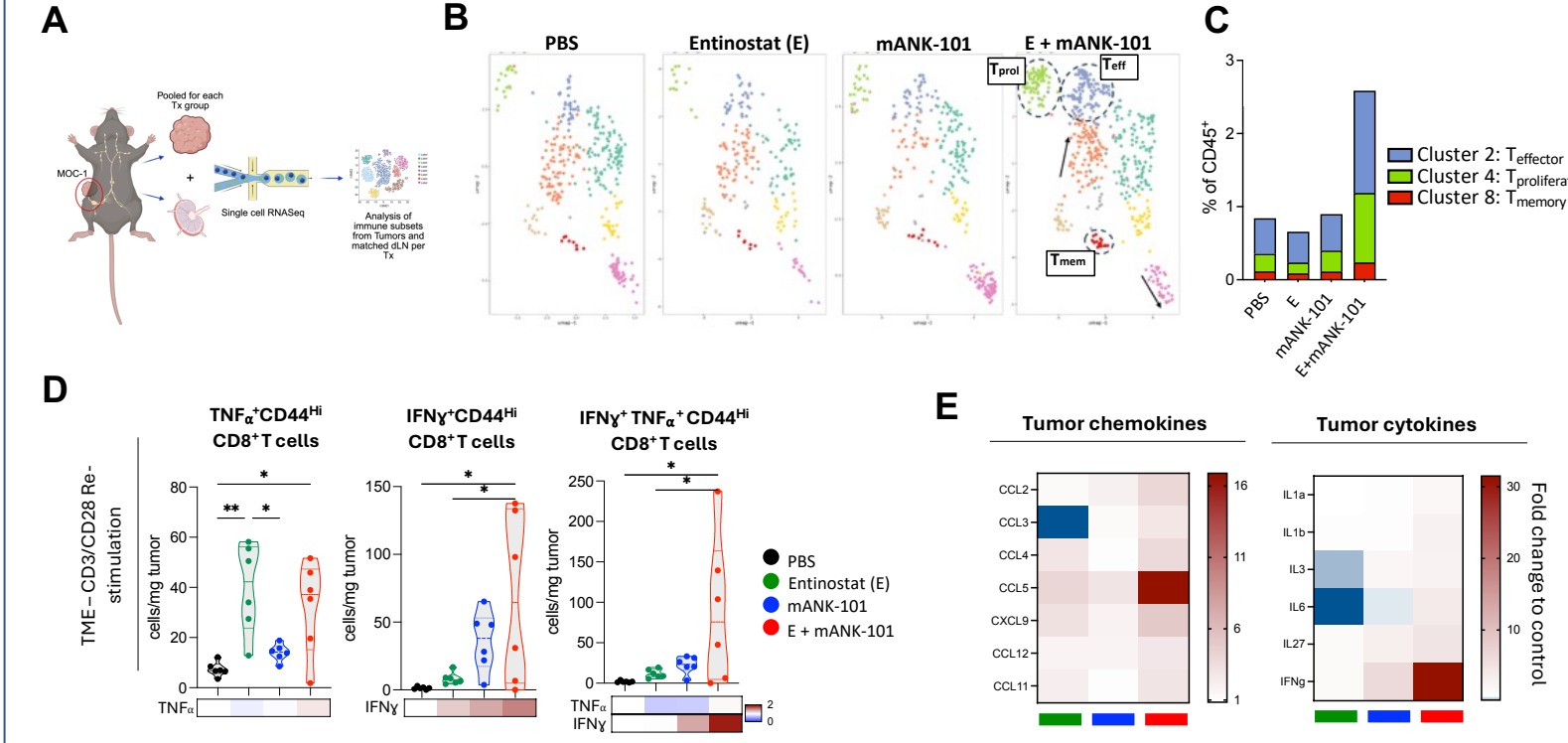


Figure 3. MOC-1 tumor bearing mice were treated as in Figure 2A and sacrificed for scRNAseq analysis. (A) scRNAseq was carried out for matched tdLN and tumors pooled per treatment and analyzed. (B) Representative UMAPs of tumor CD8⁺ T cells per treatment. (C) Clusters of effector, proliferative, and memory CD8⁺ T cells in TME as percent of CD45^{pos} cells. (D) Frequency of TNFα⁺, IFNγ⁺, and IFNγ⁺/TNFα⁺ CD8⁺ T cells in the tumor upon CD3/CD28 ex vivo stimulation. Heat maps denote respective IFNγ and TNFα gMFI fold-change versus untreated control. (E) Heatmaps show tumor chemokines and cytokines as fold changes from control (PBS) group.

4 Tertiary lymphoid structures form in response to combination therapy

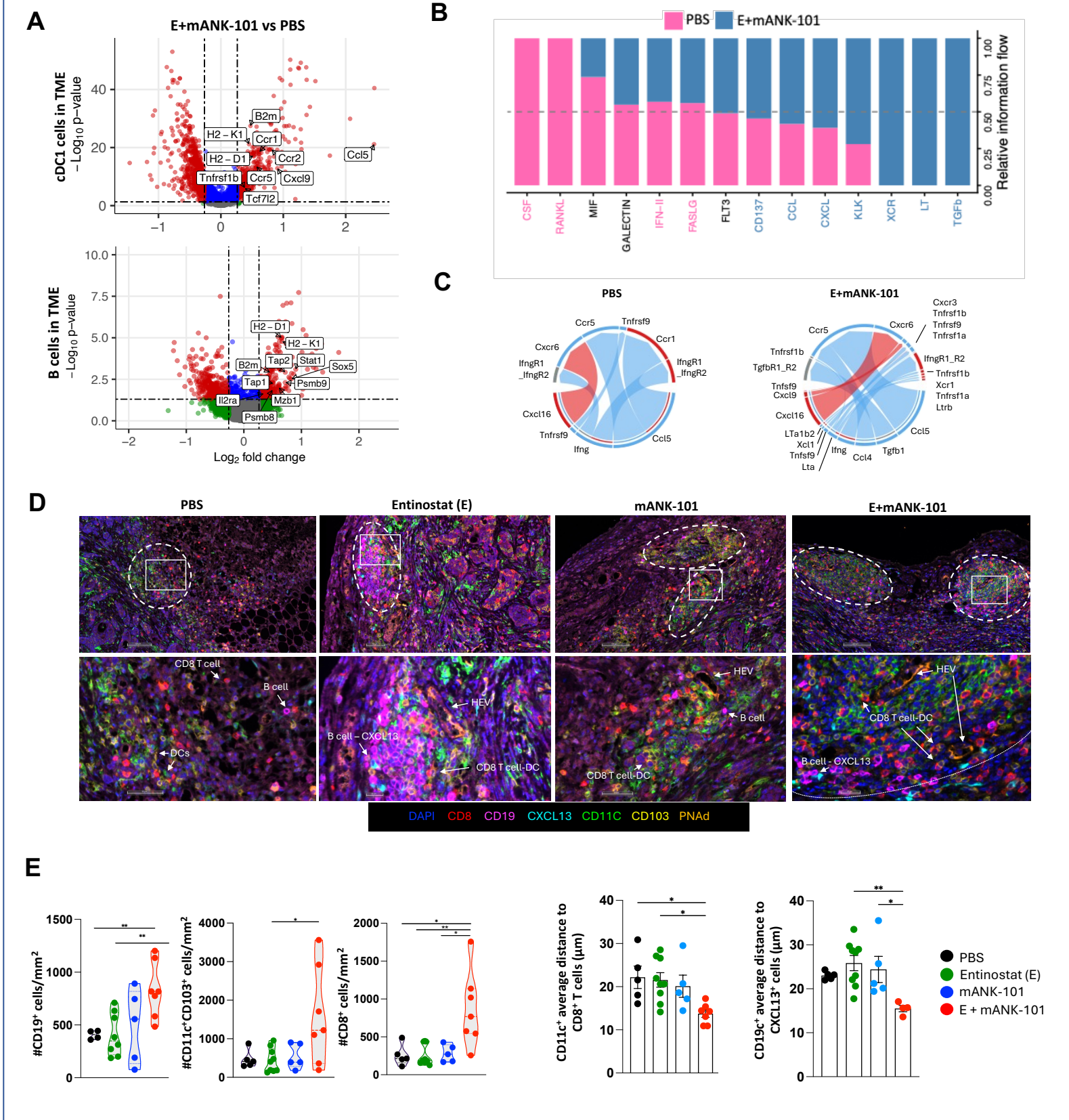


Figure 4. (A) Volcano plots show significantly expressed genes in cDC1s (top) and B cells (bottom) in the TME. Volcano plots show Entinostat (E)+mANK-101 versus PBS. Cell chat inference was applied to B, CD8 and cDC1 cells from scRNAseq. RankNet algorithm was utilized to visualize pair-wised ranked pathways (B) and genes (C) in PBS and E+mANK-101. (D) MOC-1 HPV16^{neg} tumor-bearing mice treated as in Figure 2A were examined at day 17 (4 days after mANK-101 treatment) by multiplex immunofluorescence (mIF) staining and imaging. (E) Quantification relative to figure 4D.

5 Entinostat and mANK-101 combination therapy induce stemness in CD8⁺ T cells

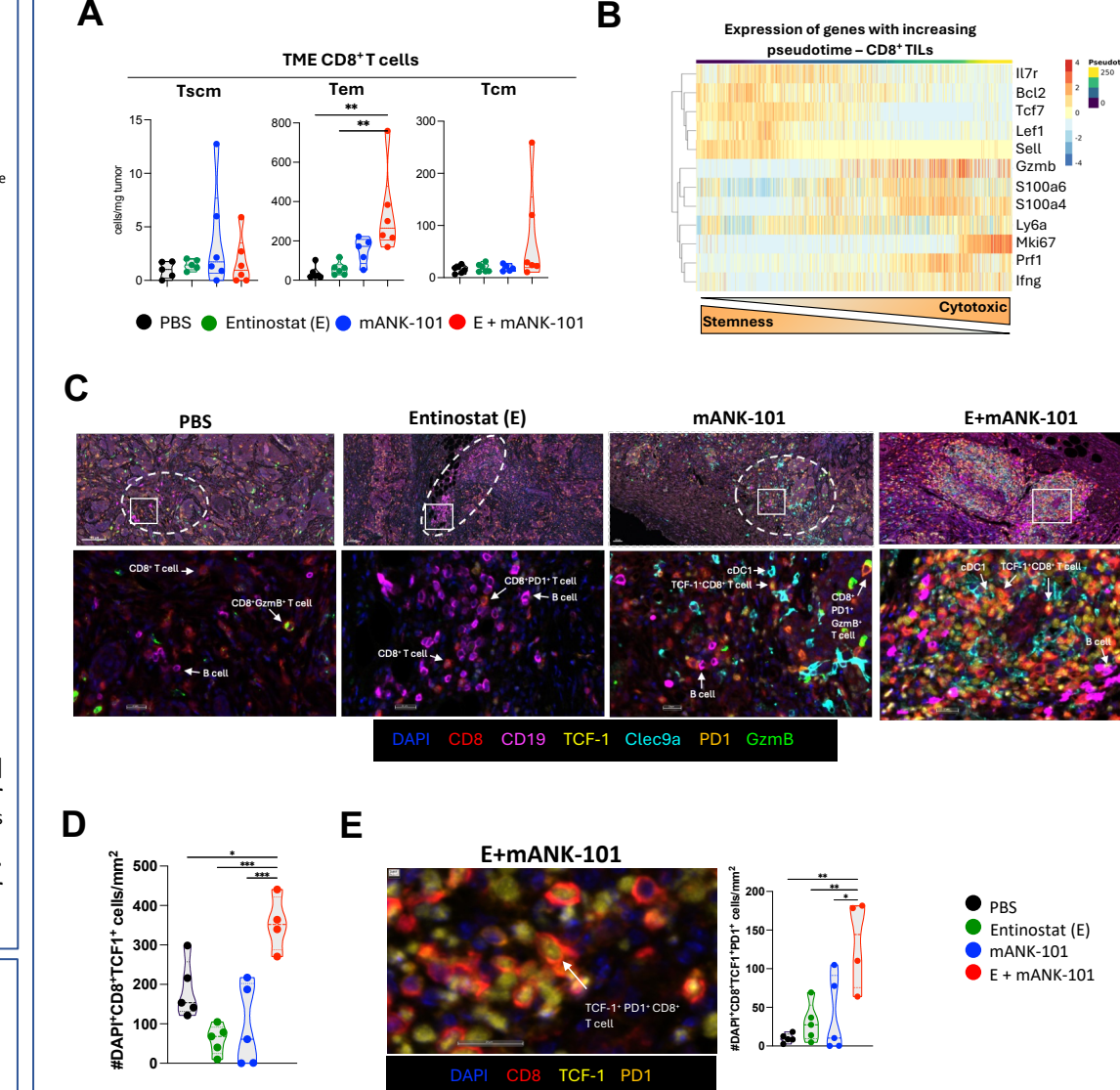


Figure 5. (A) Frequencies in the tumor of CD62L^{hi}CD44^{neg}CD127^{hi}TCF1⁺ T stem like memory (Tscm), CD8⁺CD62L^{int}CD44^{int}CD127^{int} T effector memory (Tem) and CD8⁺CD62L^{lo}CD44^{hi}CD127^{lo}TCF1⁺ T central memory (Tcm) CD8⁺ T cells. (B) Pseudotime analysis of CD8⁺ T cells progression within MOC-1 tumor. (C) Multiplex immunofluorescence (mIF) staining of MOC-1 HPV16^{neg} tumors. (D) Quantification of mIF shown in 5C. (E) mIF staining of MOC-1 HPV16^{neg} tumor treated with E+mANK-101 combination therapy, and quantification.

SUMMARY

- mANK-101 plus Entinostat modulates the tumor immune microenvironment of CPB resistant MOC-1 HPV16^{neg} murine tumors for robust anti-tumor activity driven by CD8⁺ T cells.
- Combination therapy increases tumor and peripheral pro-inflammatory cytokine milieu.
- Increased effector and stem-like TCF1⁺CD8⁺ T cells combined with cDC1s, B cells, and pro-inflammatory milieu form TLS and stem-immunity hubs.

FUTURE DIRECTIONS:

- Role of other immune cells noted increased in TME including NK, and M1 macrophage cells.
- Role of increased stem-like cells in TME.

References

- Hicks KC et al. Cooperative Immune-Mediated Mechanisms of the HDAC Inhibitor Entinostat, an IL15 Superagonist, and a Cancer Vaccine Effectively Synergize as a Novel Cancer Therapy. *Clin Cancer Res.* (2020);26(3):704-716.
- Minnar, CM et al. Tumor-targeted interleukin-12 synergizes with Entinostat to overcome PD-1/PD-L1 blockade-resistant tumors harboring MHC-I and APM deficiencies. *J Immunother Cancer* (2022); 10(6):e004561.
- Battula, S et al. Intratumoral aluminum hydroxide-anchored IL-12 drives potent antitumor activity by remodeling the tumor microenvironment. *JCI Insight* (2023); 8(23):e168224.

Acknowledgments

We would like to thank Curtis Randolph for his exceptional technical assistance on this project.